THE JOURNAL OF PHYSICAL CHEMISTRY C
A JOURNAL OF THE AMERICAN CHEMICAL SOCIETY

pubs.acs.org/JPCC

Article

Distinguishing Anionic Species That Are Intercalated in Layered Double Hydroxides from Those Bound to Their Surface: A Comparative IR Study

István Pálinkó, Pál Sipos, Ottó Berkesi, and Gábor Varga*

Cite This: J. Phys. Chem. C 2022, 126, 15254−15262

Read Online

ACCESS | Metrics & More | Article Recommendations | Supporting Information

ABSTRACT: Guest molecules in layered double hydroxides (LDHs) may be located both on the surface and in the interlayer gallery. In this work, a comparative study of various IR spectroscopic methods coupled with X-ray diffraction (XRD) is presented, which makes it possible to distinguish between the two possibilities. During the experimental work, first, CaAl-LDHs intercalated with nitrate/carbonate ions were transformed to D-gluconate- and benzoate-containing solids. Depending on the initial interlayer ion, the organic molecules may end up between the layers and/or on the surface of the LDH. The IR spectra of the specimens were recorded by using four different techniques, which are different in their penetration depth (photoacoustic spectroscopy (PAS), attenuated total reflectance (ATR), diffuse reflectance IR spectroscopy (DRIFTS), and wide angle diffuse reflectance (WA-DRIFTS)). By comparing the spectra obtained, the anionic species that are surface adsorbed to LDHs were proven to be distinguishable from those intercalated in the interlayer gallery. PAS spectra are shown to provide information about interlamellar and bulk compounds. The screening of the surface species could be performed using the WA-DRIFTS technique, while ATR and DRIFTS are capable of detecting both the surface and the bulk anions residing in the top few layers.

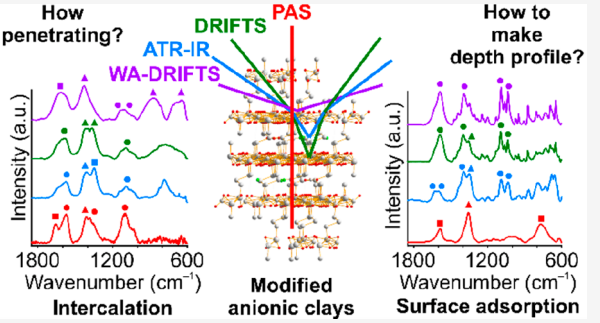

1. INTRODUCTION

Layered 2D materials have been widely studied for their unique properties, including their mechanical strength,[1] flexibility,[2] optical transparency,[3] semiconductivity,[4−6] or ability to promote atom utilization.[7−9] To use these materials in advanced hetero(nano)structures and control their bulk-scale chemical/physical properties, numerous structure modification methods have been established that would ensure the contribution of these materials to the success of materials science and electronics.[4,10−15]

To modify 2D ion-intercalated compounds, many different intercalation (wet-) chemical methods have been reported; based on these results, a large number of mixed inorganic or organo-layered composite materials were built up.[16−19] Through corresponding ion-exchange properties, these compounds can be divided into two groups, i.e., cation- and anion-exchanging materials. One of the most often used anion-exchange families is the layered double hydroxides (LDHs) in which the positive charges of the double (M^{2+} and M^{3+}) metal hydroxide layers were compensated by interlamellar solvated anions.[20,21] These interlayer anions can be further exchanged with more or less difficulties by different type of anions such as amino carboxylates,[22,23] polyoxometallates,[24] Schiff-base complexes,[25] polymeric anions,[26] DNA,[27] etc. In parallel to this process, surface adsorption of the guest molecules could also occur.[28]

In terms of their applications, it is of pivotal importance if the guest ions are situated inside or on the surface of the host (or both). For example, in order to obtain sustained drug release or contaminant sorption in a regulated way, exclusively interlamellarly modified LDH composites have to be fabricated, and the drug molecules must reside in the interlamellar space.[29,30] In contrast, by using polymers as guests, surface modification of LDH is needed for the preparation of, e.g., flame-retardant materials.[31] From an analytical point of view, the determination of the exact location of the guests is a rather challenging task. The differentiation of the guest molecules anchored to different (planar or edge-like) OH groups of the LDHs could now be achieved by combining EXAFS and atomic force microscopy (AFM) measurements.[30] This has motivated research to develop a method incorporating the comparison of IR spectra

Received: May 23, 2022
Revised: July 25, 2022
Published: September 6, 2022

recorded with various sample handling and recording methods, which is sufficient to identify the dominant local position of the guest molecules in 2D ion-intercalated composites.

For those reasons, this study is targeted at determining the local position of probe organic/inorganic (carbonate, nitrate, gluconate, and benzoate) guest molecules located in/on layered double hydroxides (LDHs), especially in/on hydrocalumites (Ca_2Al-LDH). This was achieved by comparing the spectra obtained from four different IR techniques (photoacoustic measurements (PAS); attenuated total reflection (ATR); diffuse reflection (DRIFTS); and wide-angle diffuse reflection (WA-DRIFTS)) with different penetration depth profiles.

2. EXPERIMENTAL SECTION

2.1. Materials. All the AR-grade chemical reagents were purchased from Merck and Sigma-Aldrich and used as received without further purification.

2.2. Syntheses of Pure, Intercalated, and Surface-Modified Hydrocalumites. Nitrate-intercalated hydrocalumite, $Ca_2Al(OH)_6(NO_3)\cdot nH_2O$ ($CaAl\text{-}NO_3^-$-LDH in the following), was prepared by the coprecipitation method. A mixture of $Ca(NO_3)_2\cdot 4H_2O$ (30 mmol) and $Al(NO_3)_3\cdot 9H_2O$ (15 mmol) was dissolved in 100 mL of distilled water and stirred at pH 13.1 (set by 3 M NaOH) for 12 h under a N_2 atmosphere. The slurry was filtered, washed with distilled water several times, and dried at 60 °C for 24 h in an oven.

Carbonate-intercalated hydrocalumite, $Ca_2Al(OH)_6(CO_3)_{1/2}\cdot nH_2O$ ($CaAl\text{-}CO_3^{2-}$-LDH in the followings), was produced using the dehydration−rehydration route after the same coprecipitation step as described above. An amount of 0.35 g of sodium-carbonate ($Na_2CO_3\cdot 10H_2O$) and a portion (0.75 g) of the previously heat-treated LDH (500 °C for 5 h) were suspended in an ethanol/H_2O/NaOH (1:5:1 volume ratios) mixture of 100 mL volume, and the suspension was stirred for a week at room temperature. The slurry was filtered, washed with distilled water several times, and dried in a desiccator over P_2O_5 for a few days.

The interlamellar-modified composites, denoted as CaAl-D-gluconate-LDH and CaAl-benzoate-LDH, were produced by a partial delamination-restacking method reported previously[32] that was based on the principle that nitrate ions (as opposed to carbonate ions) can be relatively readily substituted by, e.g., organic intercalants under the following experimental conditions. A portion of the previously prepared nitrate-containing LDH (0.3 g) was suspended in an EtOH/DMF mixture of 15 mL followed by a 180 min long ultrasonic treatment under a N_2 atmosphere. After the addition of 10 mL of 0.5 M Na-D-gluconate or Na-benzoate aqueous solution, the reaction mixture was stirred at room temperature for 96 h under a N_2 atmosphere. The obtained slurry was centrifuged (3000 rpm) for 15 min followed by decantation. The last two synthesis steps were repeated twice. After that, the solid product was filtered, washed with distilled water several times, and dried at 60 °C in an oven.

For the preparation of surface-modified composites, denoted as D-gluconate-CaAl-LDH and benzoate-CaAl-LDH, a portion of the previously prepared $CaAl\text{-}CO_3^{2-}$-LDH (0.3 g) was suspended in 15 mL of water followed by the addition of a 0.1 M aqueous solution of the organic-containing solutions (15 mL) into the suspension. The mixtures were stirred at 65 °C for 168 h. The obtained slurries were filtered, washed with ethanol and water twice, and dried at 60 °C for 12 h in an oven.

2.3. Characterization Techniques. Powder X-ray diffraction (XRD) patterns were recorded on a Rigaku XRD-MiniFlex II instrument applying Cu Kα radiation (λ = 0.15418 nm) at 40 kV accelerating voltage at 30 mA. The obtained materials were identified on the basis of the JCPDS (Joint Committee on Powder Diffraction Standards files) database. To determine the particle size of the composites, the samples were investigated with a scanning electron microscope (SEM, Hitachi S-4700, accelerating voltages of 10−18 kV).

The instrument for recording the IR spectra was a BIO-RAD Digilab Division FTS-65A/896 FT-IR spectrophotometer with 4 cm^{-1} resolution. Spectra in the 4000−600 cm^{-1} wavenumber range were recorded with four different detection modes (PAS, ATR, DRIFTS, and WA-DRIFTS), and 256 scans were collected for each spectrum.

Photoacoustic IR (PAS(FT-IR)) spectra of the solid samples were detected with a MTEC-200 accessory, without using any sample preparation. PAS measurements were carried out under a He atmosphere (99.99 at%), setting 2500 Hz of modulation frequency.

For attenuated total reflectance (ATR(FT-IR)) spectra, a single reflection diamond ATR accessory (SplitPea ATR Microsamplers made by Harrick) and a MCT detector were used. The application of any sample preparation process was not needed to record ATR spectra.

For diffuse reflectance spectra (DRIFTS), 1 mg of analytes was thoroughly ground with 50 mg of KBr in a mortar for 90 s. However, pure ground KBr was used as a reference for transforming the detected interferograms. DRIFTS spectra were recorded by fixing the incident angle in a 45° position. The Kubelka−Munk function was applied to convert the reflectance spectra. Constant and low concentrations of analyte guaranteed that the scattering coefficient was constant, which is a significant requirement for using the Kubelka−Munk function.

Wide-angle diffuse reflectance (WA-DRIFTS) spectra were recorded by using a Harrick variable-angle reflection accessory. To record WA-DRIFTS spectra, multilayer LDH films were deposited from ethanolic suspension on ZnSe 45° trapezoidal shaped crystals (SPT-Harrick, 50 × 20 × 2 mm) with 25 internal reflections by the dip-coating method. To ensure the smallest possible penetration depth, the non-normal incident angle (wide angle) was fixed in a constant, 78° position. Upon using this angle of incidence, no interfering effect of possible specular reflectance could be observed. Practically, hydroxyl layers of the LDH were used as a dilute sample and diffuse reflectance standard. This method was introduced on the basis of the real angular dependence of the depth penetration of the DRIFTS method.[33−35]

The surface sensitivity of the listed methods increases in the order of PAS < ATR ≤ DRIFTS < WA-DRIFTS reported previously.[19,36−45] See Table S1 for the different penetration depths from literature data associated with the FT-IR detection techniques listed above.

3. RESULTS AND DISCUSSION

3.1. Powder XRD of the LDHs. As shown in Figure 1a and b, the XRD traces of $CaAl\text{-}NO_3^-$-LDH and $CaAl\text{-}CO_3^{2-}$-LDH are identical with the patterns of the corresponding phase pure hydrocalumites published in the literature[18,46] ($CaAl\text{-}NO_3^-$-LDH: PDF#89-6723; $CaAl\text{-}CO_3^{2-}$-LDH: PDF#41-0219). The

https://doi.org/10.1021/acs.jpcc.2c03547
J. Phys. Chem. C 2022, 126, 15254−15262

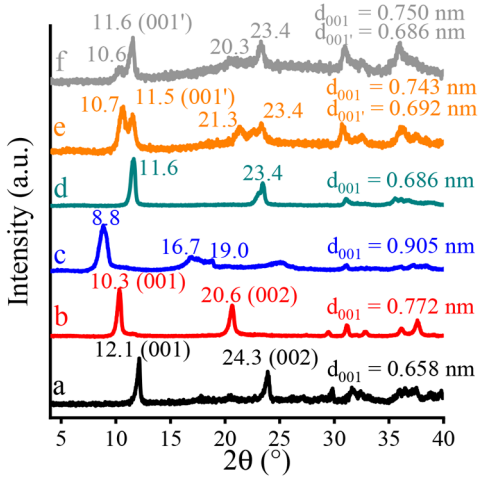

Figure 1. XRD patterns of (a) CaAl-CO_3^{2-}-LDH, (b) CaAl-NO_3^--LDH, (c) CaAl-D-gluconate-LDH, (d) D-gluconate-CaAl-LDH, (e) CaAl-benzoate-LDH, and (f) benzoate-CaAl-LDH.

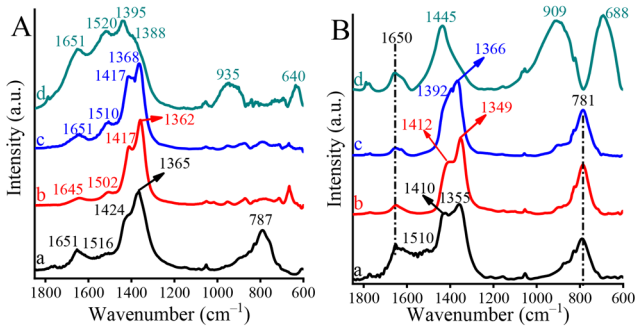

Figure 2. Midrange infrared spectra of CaAl-CO_3^{2-}-LDH (A) and CaAl-NO_3^--LDH (B) detected by different methods: PAS (a), ATR (b), DRIFTS (c), and WA-DRIFTS (d) in the range of 1850−600 cm^{-1}.

particle size of all composites can be found in Table S2. It was determined by analyzing SEM images (Figure S1). In all cases, a clear aggregation of the LDH particles can be seen, resulting in a particle size of 450−850 nm on average. The interlayer distances (d_{001}) calculated on the basis of Bragg's law are also in good agreement with the literature values. When nitrate ions are substituted with D-gluconate ions in the interlamellar space, a significant increase in the interlayer distance (from 0.772 to 0.905 nm) can be seen (compare Figure 1b with 1c); hence, the characteristic reflections of hydrocalumite are shifted toward the lower 2θ values. Upon using gluconate as the guest and carbonate-containing LDH as the host (Figure 1d), it is expected that the gluconate ions (under the experimental conditions used) are not able to displace the strongly bound carbonate ions in the interlayer gallery and are capable of adsorbing on the surface of the CaAl-CO_3^{2-}-LDH crystallites. The likely lack of intercalation is supported by the slight change of the d_{001} (from 0.658 to 0.686 nm) interlayer distance. This small difference is most probably associated with a change in the hydration of the carbonate anions in the interlayer gallery, which is known to cause small but detectable variations in the experimentally observed d_{001} values for CaAl-CO_3^{2-}-LDHs, and this value may vary between 0.66 and 0.75 nm.[47]

Clearly, the situation is much more complex for the benzoate-containing systems. The (001) reflections split for both benzoate-CaAl-LDH and CaAl-benzoate-LDH, and the calculated interlayer distances are almost identical for the two samples. Accordingly, the obtained XRD traces were not suitable for the distinction between intercalation and surface adsorption. This is in particular remarkable if we consider the already mentioned nonexchangeable character of the interlayer carbonate ions; that is, the surface adsorption of benzoate can be assumed in the case of benzoate-CaAl-LDH (see Figure 1f).

3.2. Comparison of the IR Spectra of CaAl-NO_3^--LDH and CaAl-CO_3^{2-}-LDH. By investigating these composites with the different IR spectroscopic methods, it can be noticed that the spectra of both CaAl-NO_3^--LDH and CaAl-CO_3^{2-}-LDH are strongly dependent on the spectroscopic method used (Figure 2). (For these as well as for all the further composites, the peak assignment can be found in Table S3.) In spite of the high number of analyses reported, numerous uncertainties remained in the peak assignment for IR spectra of LDHs. First, the degeneracy of the ν_3 vibration mode of carbonate ions (~1424 and 1365 cm^{-1}, Figure 2A/a−c) was able to be identified by us, similarly to literature observations, when asymmetric broadening as a result of the lowering of molecular symmetry of carbonate ions (D_{3h} to C_{2v} or C_s) was detected.[48] Besides, it was also revealed[48] that the ν_3 vibration mode of nitrate ions was not able to become degenerated as much as carbonate ions. In contrast, when nitrate is incorporated as a guest, we can observe a significant shift in its ν_3 vibrational band (~1385/1327 → 1355 cm^{-1}, Figure 2B/a-c) compared to the corresponding band positions of the previously reported surface-adsorbed nitrate ions.[49]

Effects similar to these were detected for anions intercalated into brucite-like layers, and the observations were interpreted in a variety of ways,[50−58] most often in terms of the presence of surface-bound ions. In our hands, the surface-sensitive WA-DRIFTS method proved to be a useful tool to show the vibration bands of the surface-adsorbed carbonate ions (stemming from the small amount of airborne CO_2 that is inevitably present) that appeared at 1445 (ν_3), 909 (ν_2), and 688 cm^{-1} (ν_4) (Figure 2B/d). The band positions were significantly different from those detected by the three other, more bulk sensitive IR methods in the spectra of CaAl-NO_3^--LDH; therefore, this comparative study confirms the degeneracy of the ν_3 mode of nitrate ions.[59] Similarly, the comparison of the spectra of CaAl-CO_3^{2-}-LDH provides direct proof of carbonate intercalation and surface adsorption. It can readily be seen that more than one ν_3 vibration bands (1520, 1395, and 1388 cm^{-1}) emerge in the WA-DRIFTS spectrum (Figure 2A/d). This has been most probably caused by the several possible types of coordination of CO_2 and/or carbonate on the surface of CaAl-CO_3^{2-}-LDH (due to the large concentration of carbonate ions during the synthesis of the sample). It should be noted here that the lack of the reststrahlen bands clearly confirmed that no detectable effect of the specular reflections on WA-DRIFTS spectra could be seen.[33−35] Accordingly, those are directly comparable with the results provided by other detection methods used.

Furthermore, as of yet, there is no reliable IR method to distinguish the carbonate ions from nitrate ions among the layers.[50−54,58,60−66] A large number of studies with controversial interpretation of the IR spectroscopic results regarding the proof of the incorporation of the nitrate ions were released (details are listed in Table S4).[48,50−67] However, the use of the ATR method—contrary to the others used

https://doi.org/10.1021/acs.jpcc.2c03547
J. Phys. Chem. C 2022, 126, 15254−15262

here—enables the precise distinction of these ions by providing well-separated vibration bands assigned to the (interlayer) ν_3 mode vibrations of carbonate (1362 cm^{-1}) and nitrate (1349 cm^{-1}) anions (fitted curves can be seen in Figure S2). Therefore, these results prove that it is possible to detect differences in the peak positions of the same materials using different detection methods.

The characteristic band located around 781−787 cm^{-1} does not always show up in the corresponding spectral range, raising the question whether the assignment of that band as the O−M−O bending/deformation mode is correct or not.[56,67−70] Kagunya et al. reported that there are broad and intense peaks in this spectral region due to the librational modes of hydroxyl groups and water molecules. The intensity of these bands strongly depends on the quality of the "free" water molecules capsulated in the interlayer region; nearby the surface the amount of such species may decrease.[71] Therefore, this vibration mode may be "invisible" for more surface-sensitive methods like, e.g., ATR and DRIFTS, and is clearly detectable for the more bulk sensitive PAS in the case of carbonate-containing hydrocalumite.

In the PAS spectrum of CaAl-NO_3^--LDH between 4000 and 2500 cm^{-1} (Figure 3a), two intense and more or less sharp

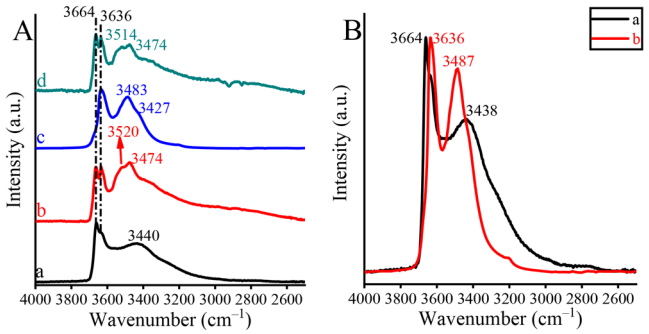

Figure 3. (A) Midrange infrared spectra between the 4000 and 2500 cm^{-1} region of CaAl-NO_3^--LDH detected by different methods: PAS (a) and WA-DRIFTS (b). The same region of CaAl-CO_3^{2-}-LDH detected by different methods: PAS (c) and WA-DRIFTS (d). (B) Comparative midrange infrared spectra between the 4000 and 2500 cm^{-1} region of CaAl-NO_3^--LDH (a) and CaAl-CO_3^{2-}-LDH (b) detected by the PAS method.

peaks (3664 and 3636 cm^{-1}), together with a broad feature at 3440 cm^{-1}, are each ascribed to the stretching mode vibrations of different types of OH groups.[66,68,70]

Unfortunately, the interpretation of this region has also been far from uniform, and there are different identifications for the absorption bands of this energy region. Considering the studies reported on hydrocalumites and Mg-based hydrotalcites, over 3600 cm^{-1}, the appearance of the well-defined peaks can be attributed to the hydroxyl groups (Ca−OH and Mg−OH) located in the octahedral layers, while the broad one under 3500 cm^{-1} is also likely to be related to hydrogen-bonded water molecules among the layers and/or on the surface.[66,68,70] Contrary to this explanation, on the basis of the cation distribution model,[72] sharp peaks—over 3500 cm^{-1}—should belong to free or defect water molecules, and bands around 3600−3500 cm^{-1} could be identified as stretching mode vibrations of bonded hydroxyl groups of the octahedral layers.[73,74] Further peaks, under 3500 cm^{-1}, were formed from the interaction between the intercalants and water molecules among the layers. Taking into account our observation that on the PAS spectrum of CaAl-CO_3^{2-}-LDH (Figure 3A/c; Figure 3B/b) significant changes in the band positions around 3600 and 3400 cm^{-1} were able to be identified in comparison to the corresponding band positions of CaAl-NO_3^--LDH (Figure 3A/a; Figure 3B/a), the cation distribution-based model seems to be more probable. Accordingly, the experienced shifts could be attributed to the variation in the composition of the interlamellar region. This assumption was strengthened by explaining WA-DRIFTS spectra of these hydrocalumites (Figure 3A/b, d). It can be seen that all vibration bands of the different hydrocalumites and their relative ratios are almost identical matches to each other. (ATR and DRIFTS spectra are not seen.) This means that there are no significant differences in the surface compositions of the hydrocalumites, being in accordance with our analyses of the fingerprint region of these LDHs.

3.3. IR Analysis of Gluconate-Containing Systems. To validate the effectiveness of the comparative IR method presented above, first, the D-gluconate-containing composites were examined, for which XRD measurements strongly support the intercalation (for CaAl-D-gluconate-LDH) or surface adsorption (for D-gluconate-CaAl-LDH) of the guest. In the fingerprint region of the intercalated CaAl-LDH (Figure 4A), the changes in the composition of the different "chops" of the composite can readily be observed; they are associated with the difference of the depth profiles.

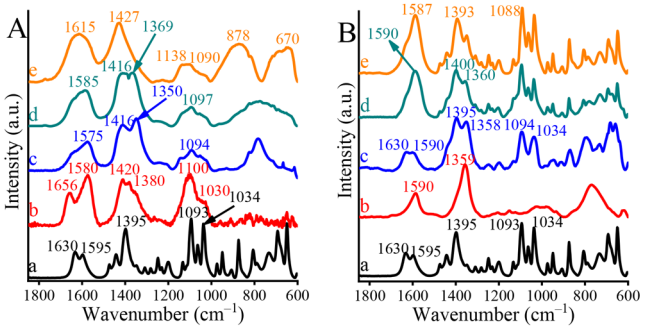

Figure 4. Midrange infrared spectra of Na-D-gluconate (PAS, a), CaAl-D-gluconate-LDH (A) and D-gluconate-CaAl-LDH (B), detected by different methods: PAS (b), ATR (c), DRIFTS (d), and WA-DRIFTS (e) in the range of 1850−600 cm^{-1}.

Several well-separated characteristic vibration peaks of the D-gluconate (at 1656, 1580, 1380, and 1100 as well as 1030 cm^{-1}) can be recorded by using PAS (compare Figure 4A/a and b).[75] It is interesting to note that by comparing to vibration bands detected on the PAS spectrum of the sodium salt of gluconate (Figure 4A/a) stretching mode vibration bands of the carboxylate group are significantly shifted, namely, 1656 ← 1630, 1595 → 1580, and 1395 → 1380 cm^{-1}. This indicates the rearrangement of the first coordination sphere of the environment of this functional group. This also means that notable ionic interactions exist between the layers and the guest due to the intercalation. Upon using ATR or DRIFTS detection modes (Figure 4A/c,d), the intensity of the characteristic bands of gluconate seems to be significantly reduced compared with the PAS results, while the stretching mode (ν_3) vibrations of the nitrate anions emerged (1350−1370 cm^{-1}). This is clearly due to the partial anion exchange which is regarded as a general phenomenon for hydro-

https://doi.org/10.1021/acs.jpcc.2c03547
J. Phys. Chem. C 2022, 126, 15254−15262

calumites. Overall, ATR or DRIFTS, having more surface-sensitive character than PAS, presents evidence for the vertical alteration of the concentration of gluconate among the layers and reflects that intercalation takes place exclusively (and not adsorption) in this case. This assumption is further strengthened by the results from WA-DRIFTS (Figure 4A/e), in which characteristic vibrations of airborne, adsorbed carbonate (1427, 878, and 670 cm^{-1}) could be detected in parallel with the almost complete disappearance the vibration bands corresponding to the D-gluconate (the respective fitted curves are shown in Figure S3).

The IR spectra of the supposedly surface-modified hydrocalumite, D-gluconate-CaAl-LDH, can be interpreted as follows. The PAS spectrum (Figure 4B/b) consisted of a well-known vibrational peak of intercalated carbonate ions (1359 cm^{-1}) and water molecules (1590 cm^{-1}). Given that PAS is a bulk sensitive method and the relative amount of the surface-adsorbed D-gluconate is minuscule relative to the intercalated carbonate, the PAS measurements confirm the assumption that (not surprisingly) carbonate ions were not possible to replace by the D-gluconate ions. On the ATR and DRIFTS spectra, further sharp peaks with high intensity (1630, 1395, 1094, and 1034 cm^{-1}) became dominant in line with a change in the depth profile of these methods (Figure 4B/c, d), indicating that these techniques "see" both the intercalated carbonate and the surface-adsorbed D-gluconate. Moreover, vibration bands that are reminiscent of those of the original CaAl-LDH cannot be observed on the spectrum recorded by WA-DRIFTS (Figure 4B/e), and the WA-DRIFTS spectrum of the composite provides almost the same envelope as that of the pure D-gluconate with almost identical peak positions (compare Figure 4A/a and e). Consequently, the interlamellar modification of the LDH could be excluded, so surface adsorption proved to be the most acceptable explanation (supported by XRD, too). This is the most probable process, which again reinforces the basic rule of ion exchange of LDHs that carbonate ions are the most strongly bound, and under non-extreme conditions they are not exchangeable.

After the intercalation, as detected by the PAS technique, OH stretching vibration bands of nitrate-containing hydrocalumite shown in Figure 5A/b (located at 3664, 3636, and 3440 cm^{-1}) have remained unchanged in intensity upon intercalation in the corresponding wavenumber region; however, they shifted (3686, 3583, and 3485 cm^{-1}) as shown in Figure 5A/c.[68,69] Besides these peaks, other ones regarding stretching mode vibrations of alkyl groups occurred. Due to the breadth of these bands, they overlapped with each other, resulting in a broad feature located around 3000 cm^{-1}. The WA-DRIFTS spectrum of this composite closely resembles that of hydrocalumite intercalated with carbonate (compare Figure 5A/d with Figure 5B/b), clearly indicating the presence of surface-adsorbed carbonate ions (with bands located at 3636 and 3493 cm^{-1}). (ATR and DRIFTS spectra are not seen.)

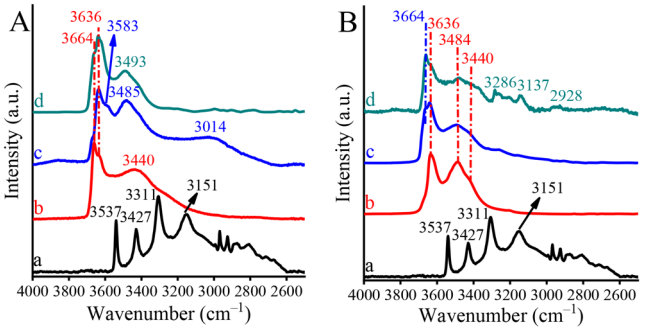

Figure 5. Midrange infrared spectra between the 4000 and 2500 cm^{-1} region of Na-D-gluconate (PAS, a) and (A) CaAl-NO_3^--LDH (PAS, b) and CaAl-D-gluconate-LDH detected by different methods PAS (c), WA-DRIFTS (d), as well as the same region of (B) CaAl-CO_3^{2-}-LDH (PAS, b) and D-gluconate-CaAl-LDH detected by different methods PAS (c) and WA-DRIFTS (d).

A trend opposite to the above one can be seen for the surface-modified composite D-gluconate-CaAl-LDH (Figure 5B/c and d). On the WA-DRIFTS spectrum (Figure 5B/d), the appearance of well-resolved peaks around 2900−3200 cm^{-1}[75] indicates the presence of a notable amount of D-gluconate physisorbed on the surface of hydrocalumite. As can be expected, the PAS spectra of CaAl-CO_3^{2-}-LDH and D-gluconate−CaAl-LDH are practically identical in this spectral range. From these, it can be concluded that the comparative method presented is suitable for distinguishing between interlamellar and surface-adsorbed anionic species.

3.4. IR Analysis of Hydrocalumites Modified by Benzoate. A comparative IR analysis on CaAl-LDHs modified by benzoate anions was also performed, with the intention of determining the limitations of the method presented in the previous section. While the XRD of D-gluconate-modified hydrocalumites gave a more or less clear picture, the XRD traces of LDHs modified by benzoate (Figure 1 e and f) are far from being obvious to interpret: neither the intercalation nor the surface adsorption of the guest was possible to verify, as a result of the occurrence of the staging effect (that is, splitting of the reflection as a result of two or more populations of interlayer structures with different interlayer distances). In the fingerprint region (Figure 6), similarly to gluconate-containing

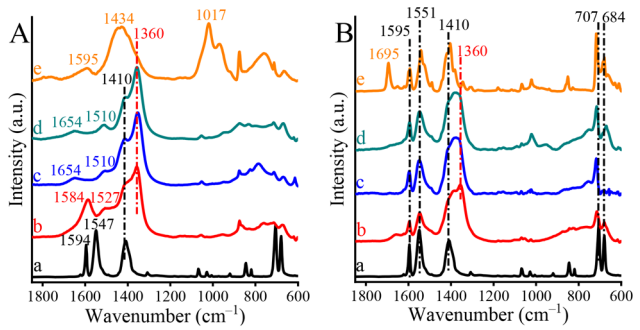

Figure 6. Midrange infrared spectra of Na-benzoate (PAS, a), CaAl-benzoate-LDH (A), and benzoate-CaAl-LDH (B) detected by different methods, PAS (b), ATR (c), DRIFTS (d), and WA−DRIFTS (e), in the range of 1850−600 cm^{-1}.

systems, two different trends could be experienced that depended on the initial LDH (NO_3^- or CO_3^{2-} containing) which determined (or at least influenced) the product of the intercalation experiment and the ultimate location of the intercalant organic anions. After treatment with benzoate, it is also assumed that a higher amount of nonexchanged initial anions remained among the layers and/or the surface compared with gluconate-containing counterparts because characteristic vibration bands of them can be located beside the characteristic peaks of the guest. The only exemption was that, by using CaAl-CO_3^{2-}-LDH as the host (Figure 6B), it is

https://doi.org/10.1021/acs.jpcc.2c03547
J. Phys. Chem. C 2022, 126, 15254−15262

clear that surface adsorption is the dominant process because of the fact that the spectrum of Na-benzoate is almost the same as the one detected on the composite by WA-DRIFTS.[76]

The spectra recorded in the high-energy region proved to be much more useful and reliable for distinguishing surface-adsorbed and interlamellar anions (Figure 7). The PAS

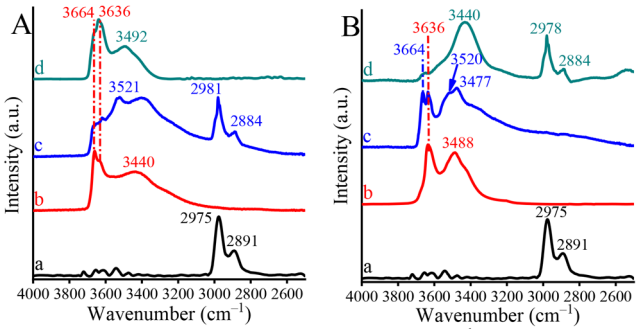

Figure 7. Midrange infrared spectra between the 4000 and 2500 cm^{-1} region of Na-benzoate (PAS, a) and (A) CaAl-NO_3^--LDH (PAS, b) and CaAl-benzoate-LDH detected by different methods, PAS (c) and WA-DRIFTS (d), as well as the same region of (B) CaAl-CO_3^{2-}-LDH (PAS, b) and benzoate-CaAl-LDH detected by different methods, PAS (c) and WA-DRIFTS (d).

spectrum of CaAl-benzoate-LDH in this spectral region clearly indicates that a significant amount of benzoate resides among the layers (Figure 7A/c) and not on the surface, as evidenced by the WA-DRIFTS spectrum (Figure 7A/d). The well-defined OH stretching vibrations of raw material significantly shifted and broadened, as a result of the increase of hydrophobicity of the interlayer gallery after intercalation.[68,69] Moreover, the characteristic features due to CH stretchings of benzoate ($\nu_{as}(CH_2)$ at 2978 cm^{-1} and $\nu_s(CH_2)$ at 2884 cm^{-1}) that appeared[76] are close those reported in the literature. The WA-DRIFTS spectrum (Figure 7A/d) attests the presence of bands of OH stretching vibrations, and some of them closely resemble those ascribed to adsorbed carbonate ions. Accordingly, the more probable explanation of these changes is that a mostly successful intercalation was achieved in this case. When one analyzes the WA-DRIFTS spectrum of the composite for which CaAl-CO_3^{2-}-LDH was used as the host (Figure 7B/d), the major difference relative to Figure 7A/d is the significant recombination of the OH vibrations of the host as well as the appearance of CH-stretching vibration bands, indicating the success of the modification of the surface with adsorbed benzoate ions. On the contrary, in accordance with our hypothesis, there have been no significant changes on the PAS spectrum of benzoate-CaAl-LDH detected (Figure 7B/c) in comparison to its carbonate-containing counterpart (Figure 7B/b). (ATR and DRIFTS spectra are not seen.)

4. CONCLUSIONS

Upon intercalation of organic hosts into CaAl-LDHs as guests via ion exchange, shifts in the positions of the characteristic reflections on the XRD traces may provide undisputable proof of the success or failure of the intercalation. However, to characterize the fine structural details, the XRD results need to be coupled with further experimental techniques. The host molecules may (or may not) reside in the interlayer gallery and/or on the surface of the LDH crystallites. A further possibility is that the original interlayer anions are only partially replaced by the guest. In some special cases, the intercalation of the host leaves the interlayer distance unaltered. In this case, XRD alone is not able to prove the success of the intercalation. The present study offers an experimental tool to distinguish among these scenarios on the basis of a detailed spectral analysis method, which is suitable for characterizing ion-intercalated and other 2D materials, especially for identifying the surface-adsorbed and the interlamellar-intercalated components.

During the work, the following strategy was followed. Intercalation of D-gluconate and benzoate as guests was attempted into CaAl-NO_3^--LDH and CaAl-CO_3^{2-}-LDH. Nitrate ions are known to be readily exchangeable, unlike carbonate ions, which can only be substituted under extreme conditions. When D-gluconate was the host molecule, from the XRD traces, it was successfully intercalated into the layers of CaAl-NO_3^--LDH, while the interlayer carbonate ions in the CaAl-CO_3^{2-}-LDH proved to be nonexchangeable. Therefore, in this case, D-gluconate ended up as surface-adsorbed anionic species. Employing benzoate as the host, the XRD results were not suitable to provide with sound interpretation. However, when the PAS, ATR, DRIFTS, and WA-DRIFTS spectra of the composites and those of the original hosts were compared, the location of the host molecules was possible to be unequivocally identified.

As a result of this, in the present publication, the comparative IR method was developed that allowed us to draw the following three major conclusions.

(i) Wide-angle diffuse reflectance infrared Fourier transform spectroscopy (WA-DRIFTS) technique is suitable for determining the adsorbed/bonded species on the surface of the layered materials without any doubt.

(ii) As a proof of concept, by comparison of the spectra obtained from surface-sensitive (WA-DRIFTS) and bulk-sensitive (PAS) methods, supplemented with two further techniques which can "see" both the surface and a few layers underneath (DRIFTS and ATR), the fact that the intercalation of the guest molecules can be strengthened or rejected regardless of the quality of the intercalant.

(iii) The fingerprint region of the IR spectra (1850−600 cm^{-1}) seems to be suitable for monitoring the fine changes of the structure of the guests associated with their interactions with the host. Conversely, the high energy region (4000−2500 cm^{-1}) is more suitable for the characterization of the spectral changes linked to the hosts, in particular, in the case of clays and clay minerals.

■ ASSOCIATED CONTENT

Supporting Information

The Supporting Information is available free of charge at https://pubs.acs.org/doi/10.1021/acs.jpcc.2c03547.

Table S1 contains the depth of penetration for the different IR methods based on the literature data; Table S2 contains the determined crystallite size of the composites; Table S3 contains the assignments of the vibration bands of the composites; and Table S4 contains the comparative literature data for band positions of ν_3 (NO_3^-) and ν_3 (CO_3^{2-}). Figure S1 shows the SEM images of the composites; Figure S2 shows the MIR fitting results of the carbonate- and nitrate-containing LDHs; and Figure S3 shows the

https://doi.org/10.1021/acs.jpcc.2c03547
J. Phys. Chem. C 2022, 126, 15254−15262

MIR—detected by PAS and WA-DRIFTS methods—fitting results of the gluconate-intercalated LDH (PDF)

AUTHOR INFORMATION

Corresponding Author

Gábor Varga − *Materials and Solution Structure Research Group, Institute of Chemistry, University of Szeged, Szeged H-6720, Hungary; Department of Physical Chemistry and Materials Science, University of Szeged, Szeged H-6720, Hungary;* orcid.org/0000-0002-7131-1629; Email: gabor.varga5@chem.u-szeged.hu

Authors

[#]István Pálinkó − *Department of Organic Chemistry, University of Szeged, Szeged H-6720, Hungary; Materials and Solution Structure Research Group, Institute of Chemistry, University of Szeged, Szeged H-6720, Hungary;* orcid.org/0000-0002-8508-309X

Pál Sipos − *Materials and Solution Structure Research Group, Institute of Chemistry, University of Szeged, Szeged H-6720, Hungary; Department of Inorganic and Analytical Chemistry, University of Szeged, Szeged H-6720, Hungary;* orcid.org/0000-0003-1407-0950

Ottó Berkesi − *Materials and Solution Structure Research Group, Institute of Chemistry, University of Szeged, Szeged H-6720, Hungary; Department of Physical Chemistry and Materials Science, University of Szeged, Szeged H-6720, Hungary*

Complete contact information is available at: https://pubs.acs.org/10.1021/acs.jpcc.2c03547

Notes

The authors declare no competing financial interest.
[#]Deceased.

ACKNOWLEDGMENTS

This work was supported by the Hungarian Government. G. Varga is grateful for the postdoctoral fellowship under the grant PD 128189. This work was also supported by University of Szeged Open Access Fund (Grant number: 5876). The financial help is highly appreciated.

REFERENCES

(1) Sangian, D.; Ide, Y.; Bando, Y.; Rowan, A. E.; Yamauchi, Y. Materials Nanoarchitectonics Using 2D Layered Materials: Recent Developments in the Intercalation Process. *Small* **2018**, *14* (33), 1800551.

(2) Seol, M.; Kim, S.; Cho, Y.; Byun, K. E.; Kim, H.; Kim, J.; Kim, S. K.; Kim, S. W.; Shin, H. J.; Park, S. Triboelectric Series of 2D Layered Materials. *Adv. Mater.* **2018**, *30* (39), 1801210.

(3) Autere, A.; Jussila, H.; Dai, Y.; Wang, Y.; Lipsanen, H.; Sun, Z. Nonlinear Optics with 2D Layered Materials. *Adv. Mater.* **2018**, *30* (24), 1801210.

(4) Stark, M. S.; Kuntz, K. L.; Martens, S. J.; Warren, S. C. Intercalation of Layered Materials from Bulk to 2D. *Adv. Mater.* **2019**, *31* (27), 1808213.

(5) Su, L.; Du, H.; Tang, C.; Nan, K.; Wu, J.; Ming Li, C. Borate-Ion Intercalated Ni−Fe Layered Double Hydroxide to Simultaneously Boost Mass Transport and Charge Transfer for Catalysis of Water Oxidation. *J. Colloid Interface Sci.* **2018**, *528*, 36−44.

(6) Li, Z.; Mu, X.; Zhao-Karger, Z.; Diemant, T.; Behm, R. J.; Kübel, C.; Fichtner, M. Fast Kinetics of Multivalent Intercalation Chemistry Enabled by Solvated Magnesium-Ions into Self-Established Metallic Layered Materials. *Nat. Commun.* **2018**, DOI: 10.1038/s41467-018-07484-4.

(7) Wang, Y.; Liu, K.; Wu, J.; Hu, Z.; Huang, L.; Zhou, J.; Ishihara, T.; Guo, L. Unveiling the Effects of Alkali Metal Ions Intercalated in Layered MnO_2 for Formaldehyde Catalytic Oxidation. *ACS Catal.* **2020**, *10* (17), 10021−10031.

(8) Ning, J.; Furness, J. W.; Zhang, Y.; Thenuwara, A. C.; Remsing, R. C.; Klein, M. L.; Strongin, D. R.; Sun, J. Tunable Catalytic Activity of Cobalt-Intercalated Layered MnO_2 for Water Oxidation through Confinement and Local Ordering. *J. Catal.* **2019**, *374*, 143−149.

(9) Ötvös, S. B.; Pálinkó, I.; Fülöp, F. Catalytic Use of Layered Materials for Fine Chemical Syntheses. *Catal. Sci. Technol.* **2019**, *9* (1), 47−60.

(10) Zhang, Y.; Tao, L.; Xie, C.; Wang, D.; Zou, Y.; Chen, R.; Wang, Y.; Jia, C.; Wang, S. Defect Engineering on Electrode Materials for Rechargeable Batteries. *Adv. Mater.* **2020**, *32* (7), 1−22.

(11) Han, T. H.; Tan, S.; Xue, J.; Meng, L.; Lee, J. W.; Yang, Y. Interface and Defect Engineering for Metal Halide Perovskite Optoelectronic Devices. *Adv. Mater.* **2019**, *31* (47), 1−35.

(12) Ambrosi, A.; Pumera, M. Exfoliation of Layered Materials Using Electrochemistry. *Chem. Soc. Rev.* **2018**, *47* (19), 7213−7224.

(13) Zhu, S.; Ji, T.; Yang, B.; Yang, Z. Preparation and Characterization of PEG/Surface-Modified Layered Double Hydroxides as a New Shape-Stabilized Phase Change Material. *RSC Adv.* **2019**, *9* (41), 23435−23443.

(14) Yang, H.; Wu, H. H.; Ge, M.; Li, L.; Yuan, Y.; Yao, Q.; Chen, J.; Xia, L.; Zheng, J.; Chen, Z.; et al. Simultaneously Dual Modification of Ni-Rich Layered Oxide Cathode for High-Energy Lithium-Ion Batteries. *Adv. Funct. Mater.* **2019**, *29* (13), 1−13.

(15) Zhu, X.; Ge, T.; Yang, F.; Lyu, M.; Chen, C.; O'Hare, D.; Wang, R. Efficient CO_2 capture from Ambient Air with Amine-Functionalized Mg-Al Mixed Metal Oxides. *J. Mater. Chem. A* **2020**, *8* (32), 16421−16428.

(16) Dang, L.; Liang, H.; Zhuo, J.; Lamb, B. K.; Sheng, H.; Yang, Y.; Jin, S. Direct Synthesis and Anion Exchange of Noncarbonate-Intercalated NiFe-Layered Double Hydroxides and the Influence on Electrocatalysis. *Chem. Mater.* **2018**, *30* (13), 4321−4330.

(17) Rives, V.; del Arco, M.; Martín, C. Intercalation of Drugs in Layered Double Hydroxides and Their Controlled Release: A Review. *Appl. Clay Sci.* **2014**, *88*−*89*, 239−269.

(18) Varga, G.; Somosi, Z.; Kónya, Z.; Kukovecz, Á.; Pálinkó, I.; Szilagyi, I. A Colloid Chemistry Route for the Preparation of Hierarchically Ordered Mesoporous Layered Double Hydroxides Using Surfactants as Sacrificial Templates. *J. Colloid Interface Sci.* **2021**, *581*, 928−938.

(19) Varga, G.; Kukovecz, Á.; Kónya, Z.; Korecz, L.; Muráth, S.; Csendes, Z.; Peintler, G.; Carlson, S.; Sipos, P.; Pálinkó, I. Mn(II)-Amino Acid Complexes Intercalated in CaAl-Layered Double Hydroxide - Well-Characterized, Highly Efficient, Recyclable Oxidation Catalysts. *J. Catal.* **2016**, *335*, 125−134.

(20) Kwok, W.; Suo, H.; Chen, C.; Leung, J.; Buffet, J.-C.; O'Hare, D. Synthesis of Dense Porous Layered Double Hydroxides from Struvite. *Green Chem.* **2021**, *23*, 1616−1620.

(21) Varga, G.; Szabados, M.; Kukovecz, Á.; Kónya, Z.; Varga, T.; Sipos, P.; Pálinkó, I. Layered Double Alkoxides a Novel Group of Layered Double Hydroxides without Water Content. *Mater. Res. Lett.* **2020**, *8* (2), 68−74.

(22) Tran, H. N.; Lin, C. C.; Chao, H. P. Amino Acids-Intercalated Mg/Al Layered Double Hydroxides as Dual-Electronic Adsorbent for Effective Removal of Cationic and Oxyanionic Metal Ions. *Sep. Purif. Technol.* **2018**, *192*, 36−45.

(23) Wang, N.; Huang, Z.; Li, X.; Li, J.; Ji, S.; An, Q. F. Tuning Molecular Sieving Channels of Layered Double Hydroxides Membrane with Direct Intercalation of Amino Acids. *J. Mater. Chem. A* **2018**, *6* (35), 17148−17155.

(24) Omwoma, S.; Chen, W.; Tsunashima, R.; Song, Y. F. Recent Advances on Polyoxometalates Intercalated Layered Double Hydroxides: From Synthetic Approaches to Functional Material Applications. *Coord. Chem. Rev.* **2014**, *258*−*259* (1), 58−71.

(25) Kirar, J. S.; Khare, S. Selective Oxidation of Ethylbenzene to Acetophenone over Cr(III) Schiff Base Complex Intercalated into Layered Double Hydroxide. *Appl. Organomet. Chem.* **2018**, *32* (8), 1−12.
(26) Tamesue, S.; Yasuda, K.; Endo, T. Adhesive Hydrogel System Based on the Intercalation of Anionic Substituents into Layered Double Hydroxides. *ACS Appl. Mater. Interfaces* **2018**, *10* (35), 29925−29932.
(27) Desigaux, L.; Belkacem, M. B.; Richard, P.; Cellier, J.; Leone, P.; Cario, L.; Leroux, F.; Taviot-Gueho, C.; Pitard, B. Self-Assembly and Characterization of Layered Double Hydroxide/DNA Hybrids. *Nano Lett.* **2006**, *6* (2), 199−204.
(28) Zhang, B.; Dong, Z.; Sun, D.; Wu, T.; Li, Y. Enhanced Adsorption Capacity of Dyes by Surfactant-Modified Layered Double Hydroxides from Aqueous Solution. *J. Ind. Eng. Chem.* **2017**, *49*, 208−218.
(29) Cao, Z.; Li, B.; Sun, L.; Li, L.; Xu, Z. P.; Gu, Z. 2D Layered Double Hydroxide Nanoparticles: Recent Progress toward Preclinical/Clinical Nanomedicine. *Small Methods* **2020**, *4* (2), 1−20.
(30) Rojo, H.; Scheinost, A. C.; Lothenbach, B.; Laube, A.; Wieland, E.; Tits, J. Retention of Selenium by Calcium Aluminate Hydrate (AFm) Phases under Strongly-Reducing Radioactive Waste Repository Conditions. *Dalton Trans.* **2018**, *47* (12), 4209−4218.
(31) Qiu, L.; Gao, Y.; Zhang, C.; Yan, Q.; O'Hare, D.; Wang, Q. Synthesis of Highly Efficient Flame Retardant Polypropylene Nanocomposites with Surfactant Intercalated Layered Double Hydroxides. *Dalton Trans.* **2018**, *47* (9), 2965−2975.
(32) Varga, G.; Kozma, V.; Kolcsár, V. J.; Kukovecz, Á.; Kónya, Z.; Sipos, P.; Pálinkó, I.; Szollosi, G. *β*-Isocupreidinate−CaAl-Layered Double Hydroxide Composites—Heterogenized Catalysts for Asymmetric Michael Addition. *Mol. Catal.* **2020**, *482*, 110675.
(33) Brimmer, P. J.; Griffiths, P. R. Angular Dependence of Diffuse Reflectance Infrared Spectra. Part II: Effect of Polarization. *Appl. Spectrosc.* **1987**, *41* (5), 791−797.
(34) Brimmer, P. J.; Griffiths, P. R. Angular Dependence of Diffuse Reflectance Infrared Spectra. Part III: Linearity of Kubelka-Munk Plots. *Appl. Spectrosc.* **1988**, *42* (2), 242−247.
(35) Brimmer, P. J.; Griffiths, P. R.; Harrick, N. J. Angular Dependence of Diffuse Reflectance Infrared Spectra. Part I: Ft-Ir Spectrogoniophotometer. *Appl. Spectrosc.* **1986**, *40* (2), 258−265.
(36) Berkesi, O.; Körtvélyesi, T.; Hetényi, C.; Németh, T.; Pálinkó, I. Hydrogen Bonding Interactions of Benzylidene Type Schiff Bases Studied by Vibrational Spectroscopic and Computational Methods. *Phys. Chem. Chem. Phys.* **2003**, *5* (10), 2009−2014.
(37) Vollmer, I.; Jenks, M. J. F.; Mayorga González, R.; Meirer, F.; Weckhuysen, B. M. Plastic Waste Conversion over a Refinery Waste Catalyst. *Angew. Chem.* **2021**, *133* (29), 16237−16244.
(38) Fina, L. J. Depth Profiling of Polymer Surfaces with FT-IR Spectroscopy. *Appl. Spectrosc. Rev.* **1994**, *29* (3−4), 309−365.
(39) Reeves, J. B.; McCarty, G. W.; Reeves, V. B. Mid-Infrared Diffuse Reflectance Spectroscopy for the Quantitative Analysis of Agricultural Soils. *J. Agric. Food Chem.* **2001**, *49* (2), 766−772.
(40) Szabó, T.; Berkesi, O.; Forgó, P.; Josepovits, K.; Sanakis, Y.; Petridis, D.; Dékány, I. Evolution of Surface Functional Groups in a Series of Progressively Oxidized Graphite Oxides. *Chem. Mater.* **2006**, *18* (11), 2740−2749.
(41) Tóth, P. S.; Janáky, C.; Berkesi, O.; Tamm, T.; Visy, C. On the Unexpected Cation Exchange Behavior, Caused by Covalent Bond Formation between PEDOT and Cl- Ions: Extending the Conception for the Polymer-Dopant Interactions. *J. Phys. Chem. B* **2012**, *116* (18), 5491−5500.
(42) Urban, M. W.; Koenig, J. L. Depth-Profiling Studies of Double-Layer PVF2-on-PET Films by Fourier Transform Infrared Photoacoustic Spectroscopy. *Appl. Spectrosc.* **1986**, *40* (7), 994−998.
(43) Wu, Y.; Sellitti, C.; Anderson, J. M.; Hiltner, A.; Lodoen, G. A.; Payet, C. R. An FTIR−ATR Investigation of in Vivo Poly(Ether Urethane) Degradation. *J. Appl. Polym. Sci.* **1992**, *46* (2), 201−211.
(44) Oelichmann, J. Surface and Depth-Profile Analysis Using FTIR Spectroscopy. *Z. Anal. Chem.* **1989**, *333* (4−5), 353−359.
(45) Forsskåhl, I.; Kenttä, E.; Kyyrönen, P.; Sundström, O. Depth Profiling of a Photochemically Yellowed Paper. Part II: FT-IR Techniques. *Appl. Spectrosc.* **1995**, *49* (2), 163−170.
(46) Periyasamy, S.; Viswanathan, N. Hydrothermal Synthesis of Hydrocalumite Assisted Biopolymeric Hybrid Composites for Efficient Cr(VI) Removal from Water. *New J. Chem.* **2018**, *42* (5), 3371−3382.
(47) Rosenberg, S. P.; Wilson, D. J.; Heath, C. A. Some Aspects of Calcium Chemistry in the Bayer Process. In *Essential Readings in Light Metals*; Springer International Publishing: Cham, 2016; pp 210−216. DOI: 10.1007/978-3-319-48176-0_28.
(48) Kloprogge, J. T.; Wharton, D.; Hickey, L.; Frost, R. L. Infrared and Raman Study of Interlayer Anions CO_3^{2-}, NO_3^-, SO_4^{2-} and ClO_4^- in Mg/Al-Hydrotalcite. *Am. Mineral.* **2002**, *87* (5−6), 623−629.
(49) Suárez-Toriello, V. A.; Santolalla-Vargas, C. E.; De Los Reyes, J. A.; Vázquez-Zavala, A.; Vrinat, M.; Geantet, C. Influence of the Solution PH in Impregnation with Citric Acid and Activity of Ni/W/Al_2O_3 Catalysts. *J. Mol. Catal. A Chem.* **2015**, *404*−*405*, 36−46.
(50) Campos-Molina, M. J.; Santamaría-Gonźalez, J.; Merida-Robles, J.; Moreno-Tost, R.; Albuquerque, M. C. G.; Bruque-Gamez, S.; Rodríguez-Castellon, E.; Jimenez-Lopez, A.; Maireles-Torres, P. Base Catalysts Derived from Hydrocalumite for the Transesterification of Sunflower Oil. *Energy Fuels* **2010**, *24* (2), 979−984.
(51) Jensen, N. D.; Bjerring, M.; Nielsen, U. G. A Solid State NMR Study of Layered Double Hydroxides Intercalated with Para-Amino Salicylate, a Tuberculosis Drug. *Solid State Nucl. Magn. Reson.* **2016**, *78*, 9−15.
(52) Okoronkwo, M. U.; Balonis, M.; Juenger, M.; Bauchy, M.; Neithalath, N.; Sant, G. Stability of Calcium-Alumino Layered-Double-Hydroxide Nanocomposites in Aqueous Electrolytes. *Ind. Eng. Chem. Res.* **2018**, *57* (40), 13417−13426.
(53) Li, D.; Yan, W.; Guo, X.; Tian, Q.; Xu, Z.; Zhu, L. Removal of Selenium from Caustic Solution by Adsorption with Ca[Sbnd]Al Layered Double Hydroxides. *Hydrometallurgy* **2020**, *191*, 105231.
(54) Gao, X.; Chen, L.; Xie, J.; Yin, Y.; Chang, T.; Duan, Y.; Jiang, N. In Vitro Controlled Release of Vitamin C from Ca/Al Layered Double Hydroxide Drug Delivery System. *Mater. Sci. Eng., C* **2014**, *39* (1), 56−60.
(55) Wongariyakawee, A.; Schäeffel, F.; Warner, J. H.; O'Hare, D. Surfactant Directed Synthesis of Calcium Aluminum Layered Double Hydroxides Nanoplatelets. *J. Mater. Chem.* **2012**, *22* (16), 7751−7756.
(56) Williams, G. R.; O'Hare, D. New Phosphonate Intercalates of $[Ca_2Al(OH)_6]NO_3{\times}H_2O$: A Synthetic and Kinetic Study. *Solid State Sci.* **2006**, *8* (8), 971−980.
(57) Muráth, S.; Somosi, Z.; Kukovecz, Á.; Kónya, Z.; Sipos, P.; Pálinkó, I. Novel Route to Synthesize CaAl- and MgAl-Layered Double Hydroxides with Highly Regular Morphology. *J. Sol-Gel Sci. Technol.* **2019**, *89* (3), 844−851.
(58) Iqbal, M. A.; Sun, L.; Lachance, A. M.; Ding, H.; Fedel, M. In Situ Growth of a CaAl-NO_3^--Layered Double Hydroxide Film Directly on an Aluminum Alloy for Corrosion Resistance. *Dalton Trans.* **2020**, *49* (13), 3956−3964.
(59) Xu, Z. P.; Zeng, H. C. Decomposition Pathways of Hydrotalcite-like Compounds $Mg_{1-X}Al_x(OH)_2(NO_3)_X{\cdot}nH_2O$ as a Continuous Function of Nitrate Anions. *Chem. Mater.* **2001**, *13* (12), 4564−4572.
(60) Milagres, J. L.; Bellato, C. R.; Vieira, R. S.; Ferreira, S. O.; Reis, C. Preparation and Evaluation of the Ca-Al Layered Double Hydroxide for Removal of Copper(II), Nickel(II), Zinc(II), Chromium(VI) and Phosphate from Aqueous Solutions. *J. Environ. Chem. Eng.* **2017**, *5* (6), 5469−5480.
(61) Domínguez, M.; Pérez-Bernal, M. E.; Ruano-Casero, R. J.; Barriga, C.; Rives, V.; Ferreira, R. A. S.; Carlos, L. D.; Rocha, J. Multiwavelength Luminescence in Lanthanide-Doped Hydrocalumite and Mayenite. *Chem. Mater.* **2011**, *23* (7), 1993−2004.

(62) Goh, K. H.; Lim, T. T.; Dong, Z. Application of Layered Double Hydroxides for Removal of Oxyanions: A Review. *Water Res.* **2008**, *42* (6−7), 1343−1368.
(63) Clark, I.; Dunne, P. W.; Gomes, R. L.; Lester, E. Continuous Hydrothermal Synthesis of Ca_2Al-NO_3 Layered Double Hydroxides: The Impact of Reactor Temperature, Pressure and NaOH Concentration on Crystal Characteristics. *J. Colloid Interface Sci.* **2017**, *504* (3), 492−499.
(64) Millange, F.; Walton, R. I.; Lei, L.; O'Hare, D. Efficient Separation of Terephthalate and Phthalate Anions by Selective Ion-Exchange Intercalation in the Layered Double Hydroxide Ca_2Al-$(OH)_6{\cdot}NO_3{\cdot}2H_2O$. *Chem. Mater.* **2000**, *12* (7), 1990−1994.
(65) Ashekuzzaman, S. M.; Jiang, J. Q. Study on the Sorption-Desorption-Regeneration Performance of Ca-, Mg- and CaMg-Based Layered Double Hydroxides for Removing Phosphate from Water. *Chem. Eng. J.* **2014**, *246*, 97−105.
(66) Granados-Reyes, J.; Salagre, P.; Cesteros, Y. CaAl-Layered Double Hydroxides as Active Catalysts for the Transesterification of Glycerol to Glycerol Carbonate. *Appl. Clay Sci.* **2016**, *132*−*133*, 216−222.
(67) Yang, M.; Tuckley, E.; Buffet, J. C.; O'Hare, D. Rapid, Efficient Phase Pure Synthesis of Ca_2AlNO_3 Layered Double Hydroxide. *J. Mater. Chem. A* **2016**, *4* (2), 500−504.
(68) Zhang, P.; Qian, G.; Shi, H.; Ruan, X.; Yang, J.; Frost, R. L. Mechanism of Interaction of Hydrocalumites (Ca/Al-LDH) with Methyl Orange and Acidic Scarlet GR. *J. Colloid Interface Sci.* **2012**, *365* (1), 110−116.
(69) Zhang, P.; Qian, G.; Cheng, H.; Yang, J.; Shi, H.; Frost, R. L. Near-Infrared and Mid-Infrared Investigations of Na-Dodecylbenzenesulfate Intercalated into Hydrocalumite Chloride (CaAl-LDH-Cl). *Spectrochim. Acta - Part A Mol. Biomol. Spectrosc.* **2011**, *79* (3), 548−553.
(70) Gevers, B. R.; Labuschagné, F. J. W. J. Green Synthesis of Hydrocalumite (Caal-Oh-Ldh) from ca(Oh)2 and Al(Oh)3 and the Parameters That Influence Its Formation and Speciation. *Crystals* **2020**, *10* (8), 1−26.
(71) Kagunya, W.; Baddour-Hadjean, R.; Kooli, F.; Jones, W. Vibrational Modes in Layered Double Hydroxides and Their Calcined Derivatives. *Chem. Phys.* **1998**, *236* (1−3), 225−234.
(72) Sideris, P. J.; Nielsen, U. G.; Gan, Z.; Grey, C. P. Mg/Al Ordering in Layered Double Hydroxides Revealed by Multinuclear NMR Spectroscopy. *Science* **2008**, *321* (5885), 113−117.
(73) Kloprogge, J. T.; Hickey, L.; Frost, R. L. The Effects of Synthesis PH and Hydrothermal Treatment on the Formation of Zinc Aluminum Hydrotalcites. *J. Solid State Chem.* **2004**, *177* (11), 4047−4057.
(74) Zhang, J.; Su, H.; Zhou, J.; Qian, G.; Xu, Z.; Xi, Y.; Xu, Y.; Theiss, F. L.; Frost, R. Mid- and near-Infrared Spectroscopic Investigation of Homogeneous Cation Distribution in $Mg_xZn_yAl_{(X+y)/2}$-Layered Double Hydroxide (LDH. *J. Colloid Interface Sci.* **2013**, *411*, 240−246.
(75) Tajmir-Riahi, H. A.; Agbebavi, J. T. Carbohydrate Interaction with Monovalent Ions. The Effects of Li^+, Na^+, K^+, NH^{+4}, Rb^+, and Cs^+ on the Solid State and Solution Structures of d-Glucono-1,5-Lactone and d-Gluconic Acid. *Carbohydr. Res.* **1993**, *241* (C), 25−35.
(76) Kubicki, J. D.; Schroeter, L. M.; Itoh, M. J.; Nguyen, B. N.; Apitz, S. E. Attenuated Total Reflectance Fourier-Transform Infrared Spectroscopy of Carboxylic Acids Adsorbed onto Mineral Surfaces. *Geochim. Cosmochim. Acta* **1999**, *63* (18), 2709−2725.

https://doi.org/10.1021/acs.jpcc.2c03547
J. Phys. Chem. C 2022, 126, 15254−15262